Neutron scattering by phonons in quasi-crystals

1990 J. Phys.: Condens. Matter 2 2519

(http://iopscience.iop.org/0953-8984/2/11/002)

J. Phys.: Condens. Matter **2** (1990) 2519–2536. Printed in the UK

Neutron scattering by phonons in quasi-crystals

C Benoit, G Poussigue and A Azougarh
Groupe de Dynamique des Phases Condensées, Unité associé au CNRS 233, Université des Sciences et Techniques du Languedoc 34095, Montpellier Cedex 5, France

Received 26 June 1989, in final form 25 September 1989

Abstract. Using the spectral moments method, we studied the inelastic scattering by phonons in very long Fibonacci chains. The results show that the pseudo-acoustic dispersion curves can be associated with Bragg peaks. The intensity of the acoustic phonon lines is proportional to the intensity of the corresponding Bragg peak. A study of disordered Fibonacci chains shows that the intensity of the phonon lines decreases strongly with increasing disorder. These results could explain the difficulties encountered in measurements of the acoustic modes in quasi-crystals.

1. Introduction

The purpose of this work is to study the inelastic neutron scattering of a quasi-crystal. We do this using the spectral moments method which permits us to obtain a differential cross section without any direct determination of eigenfrequencies or eigenvectors and which avoids the use of boundary conditions.

We show that, principally for acoustic modes, one can find some similarities between periodic and quasi-periodic systems. We also develop a method to determine directly the displacement–displacement correlation function.

As is well known, many time-independent features of the structure of solids and liquids can be studied by neutron scattering using the techniques of neutron spectrometry (Brockhouse 1966), the scattering cross section being directly related to the time-dependent density–density or Van Hove (1954) pair correlation function.

If the energy transfer occurring during the scattering is negligible compared with the energy of the scattered neutrons, for instance for a set of atoms fixed in space, the cross section is expressible in terms of the Fourier transformation of the static pair distribution $g(\boldsymbol{r})$ which describes the average density distribution as seen from a particle of the system. In liquid and dense gases, if we do not consider systems approaching critical conditions, the pair distributions exhibit short-range correlations which produce classical ring patterns, the shape, number and width of the rings depending on the type and range of correlation.

Owing to the periodicity, for a perfect crystal the range of correlation is infinite, giving rise to the concentration of the elastic scattered particles in very narrow beams (Laue Bragg reflections). If we now consider propagating density fluctuations, scattering with energy transfer occurs and the inelastic cross section is now related to the Fourier transform over space and time variables of the time-dependent pair correlation $G(\boldsymbol{r}, t)$ (Van Hove 1954). For harmonic systems and scattering with exchange of vibrational

0953-8984/90/112519 + 18 $03.50

quanta, the inelastic cross section is directly obtained from the displacement–displacement correlation function (Glauber 1955).

In a perfect crystal the displacement field can be developed in plane waves and it is easy to show that, from Bloch's theorem, the frequencies and amplitude vary periodically as the phonon wavevector $\boldsymbol{q}_{\mathrm{ph}}$ ranges through reciprocal space.

Let $\boldsymbol{G}$ be a basic vector of the reciprocal lattice; one then obtains

$$\omega_j^2(\boldsymbol{q}_{\mathrm{ph}} + \boldsymbol{G}) = \omega_j^2(\boldsymbol{q}_{\mathrm{ph}}) \qquad \forall \boldsymbol{G} \tag{1}$$

and

$$\boldsymbol{e}_j(\boldsymbol{q}_{\mathrm{ph}} + \boldsymbol{G}) = \boldsymbol{e}_j(\boldsymbol{q}_{\mathrm{ph}}) \qquad \forall \boldsymbol{G} \tag{2}$$

where $\omega_j^2(\boldsymbol{q}_{\mathrm{ph}})$ and $\boldsymbol{e}_j(\boldsymbol{q}_{\mathrm{ph}})$ are respectively the square of the frequency and the amplitude of the phonon $(j, \boldsymbol{q}_{\mathrm{ph}})$, where j is the branch index and $\boldsymbol{q}_{\mathrm{ph}}$ the wavevector.

Let $\hbar\boldsymbol{Q}_{\mathrm{d}}$ and $\hbar\omega$ be the momentum and energy transferred by the neutron to the scattering system, and $\boldsymbol{k}_0$ and $\boldsymbol{k}$ the initial and final wavevectors of the neutron. In a perfect crystal, one obtains (Brockhouse 1966)

$$\boldsymbol{Q}_{\mathrm{d}} = \boldsymbol{k}_0 - \boldsymbol{k} = \boldsymbol{G} - \boldsymbol{q}_{\mathrm{ph}} \tag{3}$$

$$\hbar\omega = \hbar^2 k_0^2/2m - \hbar^2 k^2/2m = \pm\hbar\omega_j(\boldsymbol{q}_{\mathrm{ph}}). \tag{4}$$

In (3) the $\pm$ sign for $\boldsymbol{q}_{\mathrm{ph}}$ has been omitted by restoring the range of $\boldsymbol{q}_{\mathrm{ph}}$ to the whole of the Brillouin zone. Equations (3) and (4) are a direct consequence of equations (1) and (2) and show that measurement of a given phonon can be performed, in principle, in different cells of the reciprocal lattice. This effect is a consequence of equations (2) which show that displacement–displacement correlations are identical for wavevectors which differ only by a vector of the reciprocal lattice. However, the cells of the reciprocal lattice are not strictly identical, the intensity of phonon scattering being modulated by a phase factor which depends on the structure of the unit cell.

For general systems, without any special symmetry properties, equations (3) and (4) become

$$\boldsymbol{Q}_{\mathrm{d}} = \boldsymbol{k}_0 - \boldsymbol{k} \tag{5}$$

$$\hbar\omega = \hbar^2 k_0^2/2m - \hbar^2 k^2/2m = \pm\hbar\omega_j. \tag{6}$$

$j = 1, 2, \ldots, dN$ where ω_j is the frequency of the jth mode with the amplitude $\boldsymbol{e}_j$, d is the space dimension and N the number of atoms.

Recently the discovery of the icosahedral phase (Shechtman *et al* 1984, Shechtman and Blech 1985) has shown that the strictly periodic translational symmetry is not necessary to obtain sharp diffraction peaks, the Fourier transform of almost periodic or quasi-periodic pair correlation function generating also sharp peaks (for a review see Gratias and Michel (1986) and Janot and Dubois (1988)). Spectra and wavefunctions of incommensurate and quasi-periodic crystals have been widely studied in one-dimensional model systems. Three types of model have been specially studied (Janssen 1988a): the tight-binding model with an almost periodic potential (Aubry and Andre 1979, Kohmoto 1983, Ostlund and Pandit 1984), the modulated spring model (de Lange and Janssen 1981) and the modulated Kronig–Penney models (Kollar and Suto 1986).

The studies have been performed mainly numerically on finite chains either by a periodic approximation or by the use of the transfer matrix technique. Recently multifractal properties of spectra and wavefunctions have been discussed by means of an entropy function (Kohmoto 1988, Janssen and Kohmoto 1988).

The integrated density of states (IDS) is a Cantor function and the spectra have scaling properties. The eigenstates are neither localised nor extended but 'critical', and the properties of the spectra and wavefunctions are very different from those in periodic crystals. Thus it is very interesting to study the physical properties of such systems. While many studies concern the properties of the spectra and the wavefunctions, very few consider the determination of the physical response of the systems which mainly involves the calculation of all eigenvalues and eigenfunctions. This is a difficult problem. Besides the academic interest of this study, we were directly motivated by the recent work of Janot *et al* (1988) who found difficulties, using inelastic neutron scattering techniques, in measuring acoustic modes in quasi-crystals. It will be interesting to know whether the difficulties encountered in these measurements arise from intrinsic or extrinsic (faults and disorder) properties of the materials.

In the following we shall study the inelastic neutron scattering from a quasi-crystal and analyse the behaviour of the spectrum when the range of the momentum transfer covers several Bragg diffraction peaks in the quasi-reciprocal lattice. First, we consider a perfect Fibonacci chain (FC) and then a chain with disorder. We compare the results with those obtained with a perfectly dimerised chain (PDC).

2. Models

For a review of different models used in the study of quasi-lattices, see for instance the paper of Currat and Janssen (1988 and references therein). A simple one-dimensional quasi-lattice with two basic lengths is defined by giving the location of the nth atom as (Lu and Birman 1986)

$$r(n) = s(n + \alpha[n/\sigma + \beta])/\rho \tag{7}$$

where $[x]$ represents the largest integer which is smaller or equal to x, $(\alpha, \beta) \in (0, 1)$, s is a scale factor, and σ and ρ are parameters. The lattice defined by (7) has only two nearest-neighbour spacings $a_s = s$ and $a_l = s(1 + 1/\rho)$. The average spacing a is given by

$$a = s(1 + 1/\sigma\rho). \tag{8}$$

We now assume that $\sigma = \rho = \tau = (V_5 + 1)/2$. τ is the 'golden mean'. One then obtains the Fibonacci lattice. It can be shown that the positions of the atoms are the superposition of a regular lattice with the period a modulated by a periodic function with period σa. So the FC is an incommensurate system which gives rise to Bragg reflections. It is considered a good model for quasi-periodic systems.

The Fourier transform of the Fibonacci lattice is given by (Lu and Birman 1986)

$$F(q) = \frac{1}{N}\sum_n \exp[iqr(n)]$$

$$= \sum_{m,n} \exp(iz_{m,n}) \frac{\sin(z_{m,n}/2)}{z_{m,n}/2} \Delta(qa - q_{m,n}a) \tag{9}$$

with

$$q_{m,n} = (2\pi/a)(n + m/\sigma)$$
$$z_{m,n} = (2\pi/\tilde{a})(n/\sigma - m)$$

and with

$$\tilde{a} = 1 + 1/\sigma\rho. \tag{10}$$

The differences between equation (10) of the present paper and equation (8) of the

Table 1. Positions and intensity of most intense Bragg peaks ($I/I_0 > 0.05$), for a perfect FC and for a PDC. The average atom spacing for the FC is $a = 3.6327$ Å^{-1} and the lattice parameter for the perfect chain is $a_d = 6.8819$ Å^{-1}.

			FC		PDC	
Number	m	n	Bragg peaks G_n (Å^{-1})	Intensity $I(G_n)$	Bragg peaks G_n^d (Å^{-1})	Intensity $I(G_n^d)$
1	0	0	0	1	0	1
2	1	0	1.0689	0.1127	0.9130	0.1313
3	0	1	1.7296	0.4930	1.8260	0.5437
4	1	1	2.7986	0.7726	2.7390	0.8042
5	1	2	4.5281	0.9076	3.6520	0.0076
6	2	2	5.5971	0.3225	4.5650	0.9218
7	1	3	6.2578	0.2304	5.4780	0.3702
8	2	3	7.3267	0.9638	6.3910	0.2695
9	2	4	9.0563	0.6780	7.3040	0.9696
10	3	4	10.1253	0.6032	8.2170	0.03782
11	2	5	10.7859	0.0617	9.1300	0.7119
12	3	5	11.8549	0.9860	10.0430	0.6496
13	4	5	12.9238	0.1805	10.9560	0.0674

paper of Lu and Birman (1986) arise from the presence of the scale factor s. Here $z_{m,n}$ is a dimensionless term. $F(q)$ is never equal to unity but can be very close.

As we have seen, several types of model have been used in the study of the properties of the spectra and the wavefunctions of a FC. However, it is reasonable to assume that the elastic constants depend only on the bond length, and that neighbouring sites are more strongly coupled if the distance between them is smaller. So, here, we choose the spring model with two force constants. This model is equivalent to the modulated-spring model with a discontinuous modulation function (Janssen and Kohmoto 1988). This model has been widely studied by Lu *et al* (1986), Kohmoto and Banavar (1986), Luck (1986) and Luck and Petritis (1986).

In order to obtain results which are directly comparable with experiments, we assume that we are dealing with a chain of aluminium atoms. For the elastic force constant k_1 of the short bonds, we choose the x–x force constant between nearest neighbours of the model of Walker (1956) for aluminium ($k_1 = 7.83 \times 10^3$ dyn cm^{-1}). For the long bonds we have taken the elastic constant $k_2 = \frac{1}{2}k_1$ following the work of Luck (1986) and Luck and Petritis (1986). The scale factor s is taken equal to 5 sin θ where tan $\theta = (\sqrt{5} - 1)/2$. The scale factor is 5 if we construct the FC by the projection method of a 2D square lattice with unit periodicity (Luck 1986). So the length of the short and long bonds are, respectively,

$$a_s = 5 \sin \theta$$

and

$$a_l = 5 \cos \theta.$$

We have reported in table 1 the positions $q_{m,n}$ and intensities $I(q) = |F(q)|^2$ of the 13 most intense Bragg peaks ($I(q)/I(q = 0) > 0.05$) for the FC and for the 13 first Bragg peaks of the PDC.

It is easy to realise that the short and long bonds appear, respectively, with the frequencies $t/(1 + t)$ and $1/(1 + t)$ ($t = 1/\tau = \tan \theta$). The total length l of the chain with L bonds is

Table 2. Relative intensities of Bragg peaks for several concentrations C of defects.

		Disordered FC		
		I/I_0 for the following defect concentrations C		
Number	Bragg peaks G_n (Å^{-1})	$C = 1\%$	$C = 10\%$	$C = 20\%$
1	0	1	1	1
2	1.0689	0.57	0.27	0.15
3	1.7296	0.49	0.21	0.09
4	2.7986	0.58	0.28	0.15
5	4.5281	0.83	0.43	0.22
6	5.5971	0.49	0.20	0.08
7	6.2578	0.47	0.20	0.15
8	7.3267	0.66	0.53	0.45
9	9.0563	0.57	0.26	0.14
10	10.1253	0.47	0.20	0.15
11	10.7859	0.34	0.36	0.16
12	11.8549	0.60	0.43	0.42
13	12.9328	0.57	0.25	0.13

$$l = Ls\{t/(1+t) + [1/(1+t)](1+1/\tau)\} = Ls(1+1/\tau^2) \tag{11}$$

in agreement with the definition of average spacing a (equation (8)).

In the disordered FC, we suppose that defects are randomly distributed in space. We consider defects as a change in the nature of the bond, short bonds becoming long bonds and vice versa. We have reported in table 2 the integrated intensity of principal Bragg peaks of the disordered chain for several concentrations of defects.

3. Methods of computation

Now we consider the expression for the coherent inelastic scattering cross section of slow neutrons:

$$\frac{\mathrm{d}^2\sigma}{\mathrm{d}\Omega\,\mathrm{d}\omega} = \frac{k_0}{k}\sum_j |F_j(Q_\mathrm{d})|^2 \frac{1}{2\omega_j}[(n_j+1)\delta(\omega-\omega_j) + n_j\delta(\omega+\omega_j)]. \tag{12}$$

$\omega > 0$ corresponds to neutron energy loss, and $\omega < 0$ to neutron energy gain. For a one-dimensional system, with $\boldsymbol{Q}_\mathrm{d} = Q_\mathrm{d}\boldsymbol{u}$ ($\boldsymbol{u}$ is a unit vector parallel to the chain),

$$F_j(Q_\mathrm{d}) = \sum_n b_n \exp[w(n)] \frac{e_j(n)}{\sqrt{m_n}} Q_\mathrm{d} \exp[-\mathrm{i}Q_\mathrm{d} r(n)]. \tag{13}$$

$e_j(n)$, m_n, b_n, $\exp[w(n)]$ are, respectively, the nth component of amplitude of the jth mode with frequency ω_j, the atom mass, the Fermi scattering length and the Debye–Waller factor of the nth atom; $n_j = n(\omega_j)$ is the Boltzmann factor.

Determination of (12) and (13) needs the calculation of eigenfrequencies and eigenvectors of the dynamical matrix which is not easy for large systems without perfect periodicity. Usual diagonalisation fails for systems greater than about 350 atoms, in one-dimensional space, which is very few atoms if we want, for instance, to study with accuracy the propagation of sound waves. It is possible to use a commensurate perfect lattice with a large unit cell (Janssen 1988b). However, we lose the quasi-periodicity

aspect of the system. For the problem treated here, with interaction between first neighbours only, one can use the method of transfer matrix (Lu *et al* 1986, Kohmoto and Banavar 1986, Luck 1986, Luck and Petritis 1986) although the determination of eigenvectors is not a very easy problem. As we need to calculate a great number of spectra for very large systems, we have therefore used the spectral moments method (Benoit 1987, 1989) which permits us to determine the differential cross section for systems as large as $N > 2 \times 10^6$. In this method we extract, directly from the dynamical matrix, only the active modes in the processes studied, with the correct intensity. We do not calculate those eigenfrequencies and eigenvectors of the dynamical matrix that we do not need. With this method, one determines the generalised moments of the function $S(\boldsymbol{q}, \omega)$ for $\omega > 0$ such that ($\beta = 1/kT$)

$$S(Q_d, \omega) = \frac{k}{k_0}[1 - \exp(-\beta h\omega)]\frac{d^2\sigma}{d\Omega\, d\omega}$$

$$= \sum_j |F_j(Q_d)|^2 \frac{1}{2\omega_j}[\delta(\omega - \omega_j) - \delta(\omega + \omega_j)]. \tag{14}$$

From knowledge of the moments, we calculate the scattering cross section itself. However, it is well known that the moments method presents difficulties in the low-frequency part of spectra. So, if we want to study the propagation of the sound wave, we have to check carefully the results obtained by this method.

For instance the frequency of the sound wave is about 0.06 THz for $q_{ph} = 0.01$ Å^{-1}. The maximum frequency ν_{max} is equal to 3.56 THz. As one works with the squares of the frequencies the spectral region which we are interested in lies only in a thousandth of the total spectral range. In order to test our method we have compared our results first with the results obtained by direct diagonalisation (for systems with 145 atoms, $F_1 = 12$) and secondly for longer chains (for up to 4182 atoms, $F_1 = 19$), with the results of a new method, based on the Gauss–Jordan elimination procedure. This method is developed in the appendix. Excellent agreement is obtained between the moments method and the method based on Gauss–Jordan elimination, if we use at least 100 generalised moments (figure 1). The length of the chain will be varied from 145 to 2 178 000 atoms. For more details concerning the computation procedure, see Benoit and Poussigue (1989).

4. Results

To analyse the phonon spectrum of the FC, we follow the same steps as for perfect crystals. Having computed the positions $\boldsymbol{G}_n$ of Bragg peaks (table 1), we define a vector $\boldsymbol{q}_{ph}$ such that, by comparison with (3),

$$\boldsymbol{Q}_d = \boldsymbol{k}_0 - \boldsymbol{k} = \boldsymbol{G}_n - \boldsymbol{q}_{ph}. \tag{15}$$

Here, $\boldsymbol{q}_{ph}$ is not a good quantum number and does not correspond to the pseudo-momentum of a phonon. Exception must be made for acoustic waves which correspond to a translation of the whole system and which do not depend on the particular structure of the material.

We first focus our attention on acoustic modes. We have computed the phonon spectra near every Bragg peak for a momentum transfer such that q_{ph} has a constant value equal to 0.005 Å^{-1}. We obtain, for the 13 spectra, exactly the same shape (figure

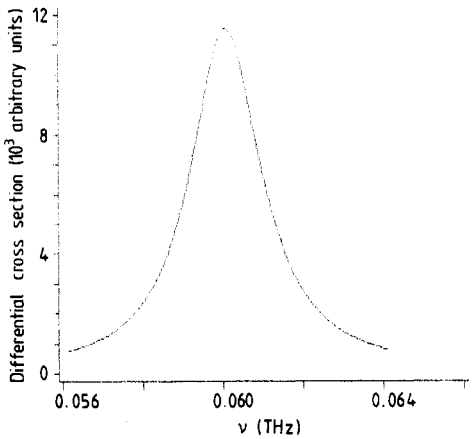

Figure 1. Detail of the low-frequency part of the differential cross section of a FC ($N = 4182$ atoms; $F_l = 19$) calculated with 100 moments for $Q_d = 4.518\,17$ Å^{-1}, $G_5 = 4.528\,17$ Å^{-1} and $q_{ph} = 0.01$ Å^{-1}. The exact value of ν_s is 0.060 078 THz, and the calculated value of ν_s is 0.060 08 ± 0.000 04 THz. The CPU time is 5.83 s.

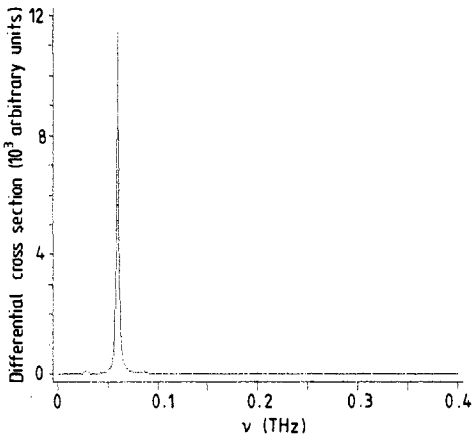

Figure 2. Low-frequency part of the differential cross section of a FC ($N = 4182$ atoms; $F_l = 19$) calculated with 100 moments for $Q_d = 4.518\,17$ Å^{-1}, $G_5 = 4.528\,17$ A^{-1} and $q_{ph} = 0.01$ Å^{-1}.

2); a strong peak appears, with exactly the same frequency in each spectrum. To be sure that the observed peaks arise from acoustic modes we used two types of test: first we checked that the frequency of peaks varies linearly with the wavevector $q_{ph} = G_n - Q_d$; secondly we compared the calculated value of the velocity of sound with the exact value which can be determined theoretically in a FC. The velocity of sound is given in a linear chain by

$$v = \sqrt{C/\rho} \tag{16}$$

where C is the elastic constant and $\rho = m/a$ the specific mass.

If u_{xx} is the deformation tensor we have

$$\sigma_{xx} = Cu_{xx} \tag{17}$$

where σ_{xx} is the stress-tensor and $u_{xx} = \mathrm{d}U_x(r)/\mathrm{d}r_x$. $U_x(r)$ is the displacement of point r under the stress σ_{xx}. Under stress the length of each bond increased by $\mathrm{d}l_i$ such that $\mathrm{d}l_i = \sigma_{xx}/k_i$. The total length variation of the chain is given by

$$u_{xx} = \sum_i \mathrm{d}l_i = \sum_i \frac{1}{k_i}\sigma_{xx} = \left(\frac{n_s}{k_1} + \frac{n_l}{k_2}\right)\sigma_{xx} \tag{18}$$

where n_s and n_l are the number of short and long bonds, respectively. From (11) and (18), one obtains

$$u_{xx} = (n_s/k_1 + n_l/k_2)\sigma_{xx}\{r/s[n_s + n_l(1 + 1/\tau)]\} \tag{19}$$

where $r = l$ is the length of the chain and from (11), (16), (17) and (19) one obtains for the velocity of sound

$$v = a\sqrt{(1+t)K/m}$$

with

$$1/K = t/k_1 + 1/k_2. \tag{20}$$

Let us remark that for a perfectly dimerised chain, with $a_d = a_l + a_s$ as the lattice parameters, and k_1 and k_2 as the elastic constants, one obtains

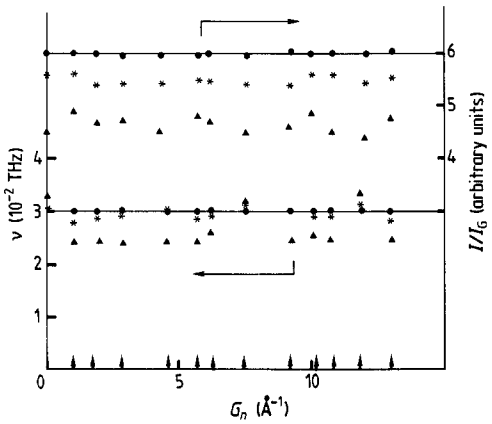

Figure 3. Results for several sample lengths: ▲, $N = 611$ atoms; *, $N = 1598$ atoms; ●, $N = 4182$ atoms. The upper part of the figure shows the ratio of intensity of the acoustic phonon lines ($q_{ph} = 0.005$ Å^{-1}) to the intensity of the corresponding Bragg peaks, and the lower part the calculated positions of the acoustic phonon lines ($q_{ph} = 0.005$ Å^{-1}; exact value $\nu = 3.0039 \times 10^{-2}$ THz). The results do not change for chains with size greater than $N = 4182$.

$$v_d = a_d\sqrt{K_d/m}$$

with

$$1/K_d = 1/k_1 + 1/k_2. \tag{21}$$

With the numerical values used here, one obtains $v = 377\,481$ cm s^{-1} and $v_d = 371\,338$ cm s^{-1}.

One finds that the position of the low-frequency peak (figure 1) agrees perfectly with the theoretical values $\nu = vq_{ph}/2\pi$.

The same results are obtained for every Bragg peak, the intensity of the acoustic phonon lines being proportional to the intensity of the corresponding Bragg peaks (figure 3). Identical results are obtained with the PDC. The length of the FC used for the calculation is equal to or higher than 4182 atoms. For shorter chains, the position and intensity of the phonon peaks are dependent on Bragg peaks and chain length (figure 3).

It is known that in a FC a crossover between two regimes appears at the value of ν for which the size l is of the order of magnitude of the length ξ such that

$$\xi = \exp(C/\nu) \tag{22}$$

where C is a constant for a given force model (Luck and Petritis 1986). For $l \ll \xi$ the states (eigenmodes) behave as Bloch states while for $l \gg \xi$ the states are in critical regime. For the acoustic modes considered here, we are therefore dealing with Bloch states, for all l, and the dependence of the position and intensity of the phonon peaks with the length of the chain arises from classical boundary effects.

We show in figures 4 and 5 the positions and intensities of phonon peaks for the FC for a momentum transfer such that $G_4 < Q_d < G_5$ (figure 4) and $G_9 < Q_d < G_{10}$ (figure 5).

For comparison we have also calculated the positions and intensities of phonon peaks for the PDC with $G_4^d < Q_d < G_5^d$ (figure 6).

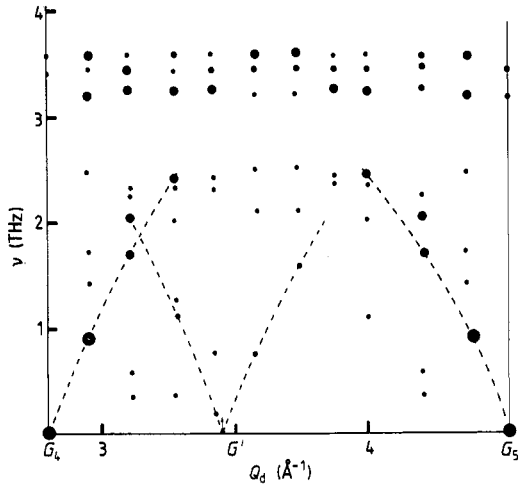

Figure 4. Pseudo-dispersion curves of a FC calculated by the spectral moments method with 100 moments for Q_d lying between the two strong Bragg peaks G_4 and G_5. G' is a Bragg peak of intensity less than $0.05I_0$. The intensities of the peaks are suggested by the dimensions of the dots.

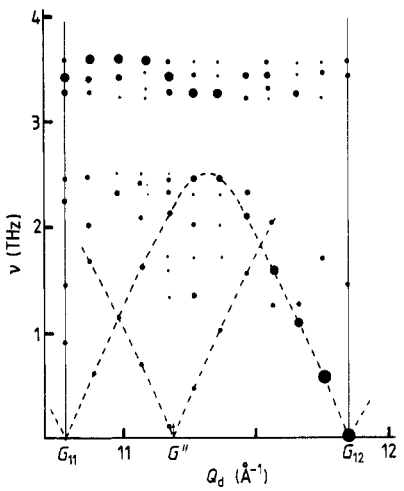

Figure 5. Pseudo-dispersion curves of a FC calculated by spectral moments method with 100 moments for Q_d lying between the two strong Bragg peaks G_{11} and G_{12}. G'' is a Bragg peak intensity less than $0.05I_0$. The intensities of the peaks are suggested by the dimensions of the dots.

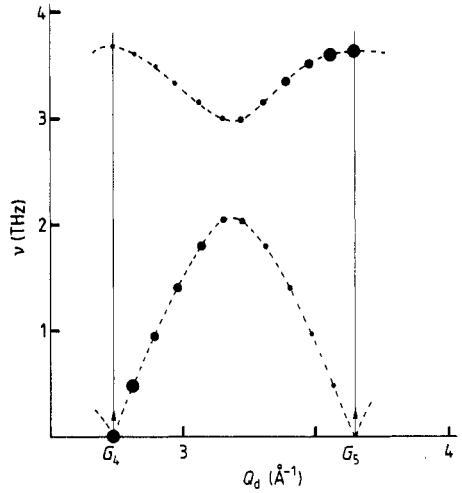

Figure 6. Dispersion curves of a dimerised chain ($N = 4182$ atoms) calculated by spectral moments method with 100 moments. The intensities of the peaks are suggested by the dimensions of the dots.

It is easy to show that the differential cross section follows a sum rule for a given Q_d. From (13) and (14) one obtains using the closure properties of eigenvectors:

$$\int_0^\infty S(Q_d, \omega) 2\omega \, d\omega = \int_0^\infty \bar{S}(Q_d, u) \, du = NQ_d^2 \frac{b^2 \exp(-2w)}{m}$$

with

$$\bar{S}(Q_d, u) = \sum_j |F_j(Q_d)|^2 \delta(u - \lambda_j) \tag{23}$$

where $u = \omega^2$ ($\omega > 0$), $\lambda_j = \omega_j^2$, $b = b_n$ $w = w(n)$ and $m = m_n \, \forall \, n$.

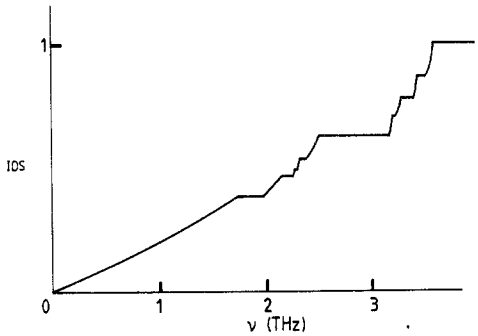

Figure 7. IDS of a FC with $m = 26.98$ g, $k_1 = 7.83 \times 10^3$ dyn cm^{-1} and $k_2 = k_1/2$.

Thus near strong (weak) Bragg peaks we must obtain strong (weak) acoustic phonon lines and weak (strong) optical phonon lines. We observe in figures 4–6 that the spectra are in good agreement with this sum rule. Pseudo-acoustic dispersion curves are associated with every Bragg peak. However, let us remark that the curves obtained are not equivalent to the classical dispersion curves obtained in perfect crystal. We show in figure 7 the IDS. Its most characteristic point is the presence of gaps at all frequencies. In other words the spectrum has no absolutely continuous component. However, in the spectral moments method, one introduces an imaginary part in the frequency (Benoit 1987). This quantity may represent the finite lifetime of phonons and/or the finite resolution of the apparatus. So the small gaps, which may not be experimentally distinguishable, are smoothed, giving rise to a low-frequency quasi-continuous acoustic dispersion curve.

In addition, we observe an acoustic peak if the momentum transfer is such that the frequency deduced from the pseudo-dispersion curves lies in a gap. In regions of reciprocal space where it is not possible to define a dispersion curve (see for instance the centre of figure 4), there are no acoustic modes but strong optical modes. Another important difference compared with the periodic lattice arises from the nature of the Fourier transform of the density function.

We know that Bragg peaks are dense in reciprocal space and we have seen that we can attribute a set of pseudo-acoustic dispersion curves to every Bragg peak. Thus, for a given momentum transfer Q_d, one obtains an infinity of phonon lines corresponding to the infinity of Bragg peaks (for an infinite FC). However, their intensity is generally very weak. We can see in figures 4 and 5 that, for instance, the frequencies of some weak peaks agree very well with pseudo-dispersion curves which can be attributed to Bragg peaks G' (figure 4) and G'' (figure 5). These peaks have not been taken into account until now, their intensity being less than 5% of intensity of the central ($Q_d = 0$) Bragg peak.

In the 'optical' region, several peaks appear. Their frequencies do not behave in a clear way. The positions found for different momentum transfers correspond to 3.20, 3.24, 3.26, 3.28, 3.42, 3.44, 3.54 and 3.56 THz. The boundaries of the principal phonon bands, in this region, are found at 3.18–3.20, 3.22–3.28, 3.38–3.44 and 3.50–3.56 THz. Thus the frequencies of these phonon peaks correspond more generally to the high-frequency side of the phonon bands. The same types of result are found with peaks in the 2–2.5 THz region. Peaks found at 2.18, 2.32 and 2.50 THz correspond to the upper part of the phonon bands. However, the peak at 2.42 THz corresponds to the centre of a phonon band (figure 7). These results could be compared with the rough empirical rule of Luck and Petritis (1986) who find that, the farther a state is from the large gaps

in the spectrum, the more it looks like a localised state. So the more intense phonon peaks should arise generally from the less localised states.

In order to obtain more information on the dynamics of the system we show in figures 8 and 9 the Fourier transform of the displacement–displacement correlation function $\langle U_n(t)U_{n'}(0)\rangle$.

The method used to obtain these quantities is based on Gauss–Jordan elimination

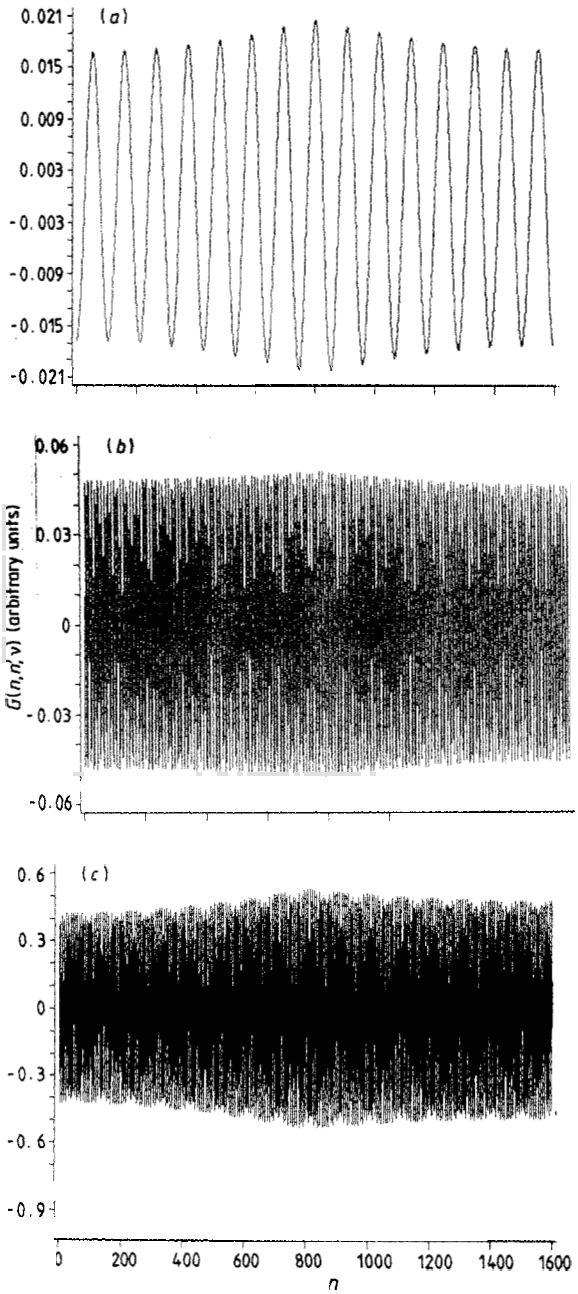

Figure 8. Fourier transform over time $G(n, n', \nu)$ of the displacement–displacement correlation function $\langle U_n(t)U_{n'}(0)\rangle$ calculated for a dimerised chain (N = 1598 atoms) by the Gauss method with $n = 799$ and $\gamma = 2 \times 10^{-3}$ THz; (*a*) ν = 0.1 THz; (*b*) $\nu = 1$ THz; (*c*) ν = 3.56 THz.

and is developed in the appendix. This method can be applied with any type of system and is very efficient.

In figure 8 we show, for comparison, the results obtained with the PDC. The results for the FC are shown in figure 9. These quantities do not represent particularly the states of the system. The physical interpretation of these correlation functions is simple only in the classical limit, when they become real.

$\langle U_n(t)U_{n'}(0)\rangle$ gives a measure of the extent to which the displacement of the atom n at time t is influenced by the fact that the atom n' suffered a displacement $U_{n'}$ at time

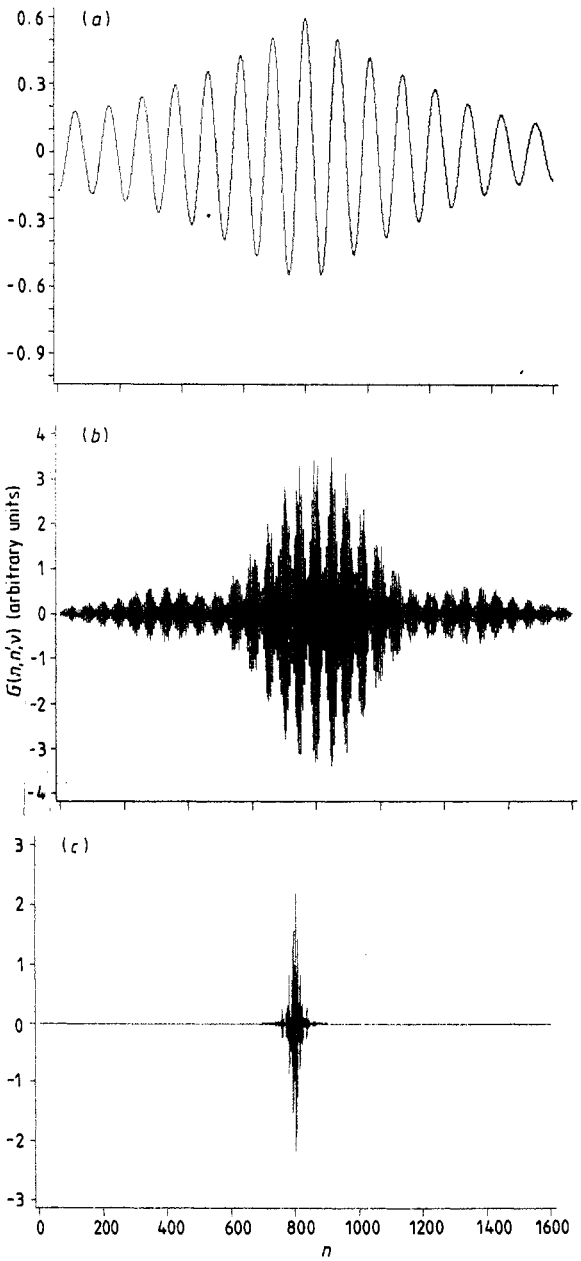

Figure 9. Fourier transform over time $G(n, n', \nu)$ of the displacement–displacement correlation function $\langle U_n(t)U_{n'}(0)\rangle$ calculated for a FC chain ($N = 1598$ atoms; $F_l = 17$) by the Gauss method with $n = 799$ and $\gamma = 2 \times 10^{-3}$ THz: (*a*) $\nu = 0.1$ THz; (*b*) $\nu = 1.7$ THz; (*c*) $\nu = 3.56$ THz.

zero. For the PDC (figure 8) the motion is not localised whatever the frequency while for the FC we observe that the localisation of motion increases as the frequency increases.

Figures 8 and 9 have been obtained with the same value of the phonon lifetime γ (see (A4)). If γ is large enough, several modes with neighbouring frequencies can be involved in the calculation of the correlation functions, giving rise to a rapid decrease due to the interference. However, if γ is small, only one mode will be involved in the summation over j in equation (A10) and one obtains the corresponding eigenvectors. The results for two values of γ are shown in figure 10 for $\nu = 1.7$ THz for a chain with 4182 atoms ($F_l = 19$). Figures 9(b) and 10(a) obtained with the same value of γ show that no large change occurs for higher N. Figure 10(b) does not change for smaller γ and so we believe that it represents the eigenstates for this frequency. This result is not in contradiction with previous works on this subject. The most interesting result is that, in quasi-crystals, the presence of very small damping yields a strong localisation of the motion. This effect is significant even at low frequencies (figure 9(a)) and has certainly large consequences on transport properties, for instance.

We discuss now the dynamics of a disordered FC. We recall that we consider a change in the nature of the bonds as disorder. We have shown in table 2 the variation in the

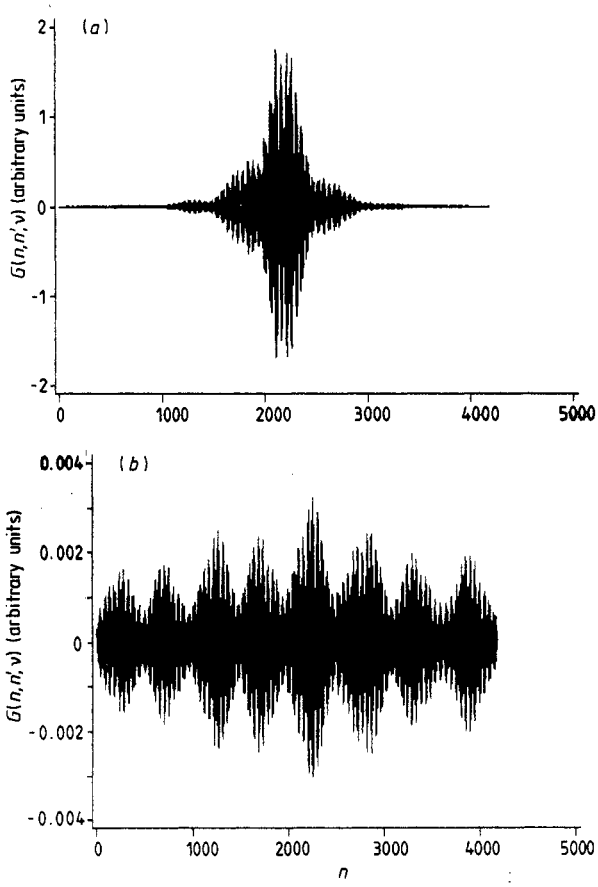

Figure 10. Fourier transform over time $G(n, n', \nu)$ of the displacement–displacement correlation function $\langle U_n(t)U_{n'}(0)\rangle$ calculated for a FC ($N = 4182$ atoms; $F_l = 19$) by the Gauss method with $n = 2091$ and $\nu = 1.7$ THz: (a) $\gamma = 2 \times 10^{-3}$ THz; (b) $\gamma = 2 \times 10^{-6}$ THz.

intensity of the Bragg peaks for several values of the disorder C, which is the ratio of the number of modified bonds to the total number of bonds. Bonds are randomly changed. This procedure does not produce a genuine disordered system; we see that, if we change, for instance, all bonds ($C = 1$), we again obtain a FC. We observe several effects; the positions of the Bragg peaks are slighly shifted while their intensity decreases strongly. However, the decrease strongly depends on the peaks; for instance very strong peaks decrease much less than weak peaks.

Examples of the differential cross section for a perfect FC and a disordered FC are shown in figures 11 and 12. We observe a large decrease in the intensity of the peaks associated with an increase in their width. We observe also the appearance of new peaks in the spectrum. Several peaks are located in the gaps of the perfect FC; others appear with frequencies higher than the maximum frequency (3.56 THz) of the perfect FC.

The change in the intensity of acoustic and optic modes with increasing disorder is shown in figure 13. We observe that the intensity of the acoustic modes decreases strongly with increasing disorder. The change is weaker for the 'optical' modes. The difficulties encountered in the measurements of acoustic modes in neutron scattering experiments

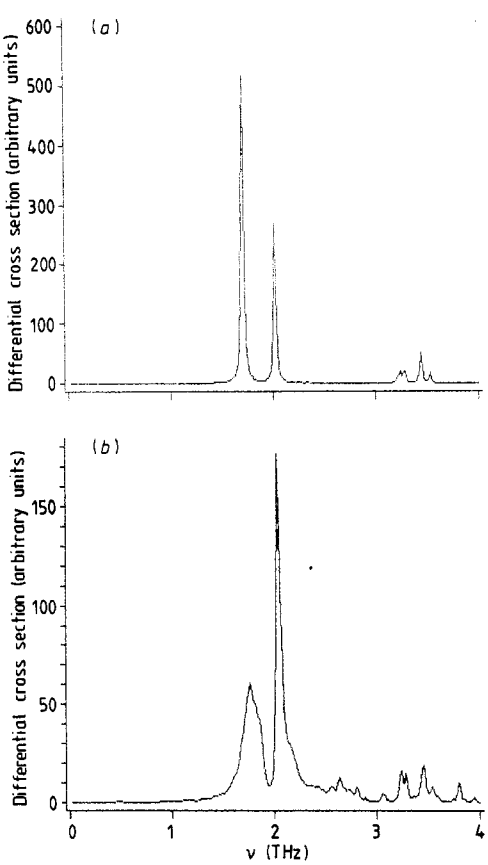

Figure 11. Differential cross section calculated with 100 moments for $Q_d = 4.2138$ Å^{-1}, $G_5 = 4.5282$ Å^{-1} and $q_{ph} = 0.3144$ Å^{-1}: (*a*) perfect FC ($N = 4182$ atoms); (*b*) disordered ($C = 20\%$) FC ($N = 4182$ atoms).

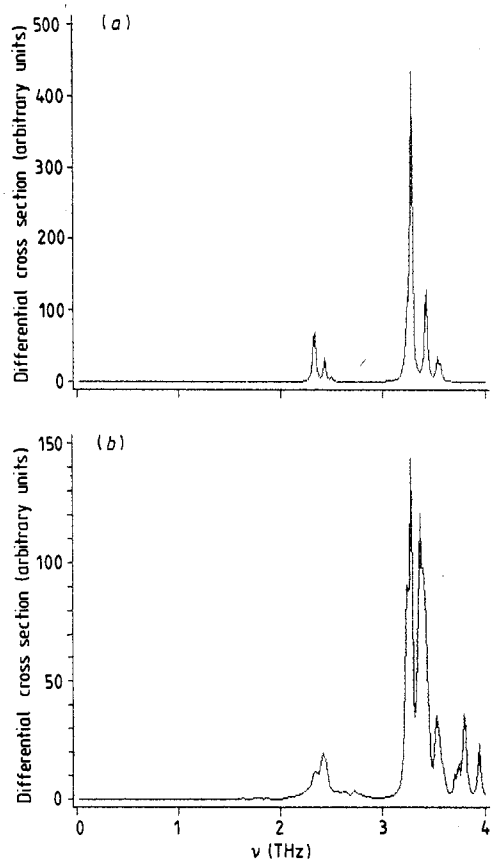

Figure 12. Differential cross section calculated with 100 moments for $Q_d = 3.8993$ Å^{-1}, $G_5 = 4.5282$ Å^{-1} and $q_{ph} = 0.6289$ Å^{-1}: (*a*) perfect FC ($N = 4182$ atoms); (*b*) disordered ($C = 20\%$) FC ($N = 4182$ atoms).

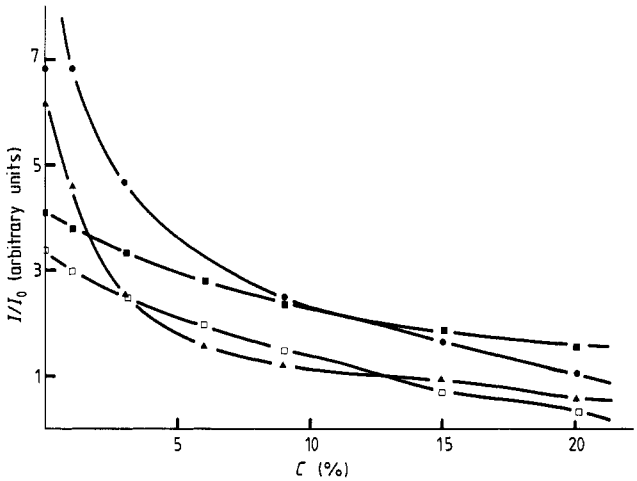

Figure 13. Variation in the ratio of intensity of some phonon lines to the intensity of the corresponding Bragg peaks for several values of disorder: ●, $Q_d = 4.371$ Å^{-1}, $\nu = 0.94$ THz; ▲, $Q_d = 4.210$ Å^{-1}, $\nu = 1.70$ THz; □, $Q_d = 4.058$ Å^{-1}; $\nu = 2.44$ THz; ■, $Q_d = 3.584$ Å^{-1}; $\nu = 3.54$ THz.

can therefore be explained by the presence of disorder which destroys the pseudo-similarity, in quasi-crystals, between the different zones of the reciprocal space.

5. Conclusion

The present work shows that neutron scattering by phonons in quasi-crystals has very interesting features. We have shown that it is possible to define for the stronger Bragg peaks pseudo-Brillouin zones which play a role highly analogous to the Brillouin zones of perfect crystals. For instance the phonon spectra present a great similarity between different zones, although their widths are often very different. Another interesting result is the possibility of measuring acoustic dispersion curves near strong Bragg peaks although the system exhibits very particular spectra and wavefunctions. The most surprising is that these dispersion curves can be followed very far from the Bragg peaks and that the intensity of the phonon lines does not present any drastic change as we go away from the Bragg peak. From the neutron scattering point of view there is no evidence of critical properties of the eigenstates. However, because the spectrum is a Cantor set, it is not possible to consider these curves as equivalent to classical dispersion curves of perfect crystals. From the correlation function we have shown that the eigenstates are certainly neither extended nor localised in the usual sense and that transport properties are certainly strongly dependent on the damping of vibrations.

Concerning the measurement of acoustic phonons we have shown that, to obtain good results, it will be necessary to choose a region of reciprocal space near a strong Bragg peak and more exactly between two strong Bragg peaks. So the method of study of a quasi-crystal is identical with the methods used with perfect systems and the difficulties in the measurements of acoustic phonons arises certainly, as we have shown, from disorder. However the model developed here is 1D and it is necessary to develop a 3D model.

Acknowledgments

We thank C Janot, R Currat and M de Boissieu of Institute Laue–Langevin (Grenoble) for stimulating discussions and helpful remarks on this work.

Appendix. Direct inversion method

A1. Calculation of the response function

We develop here another method which can be used to determine the spectra of non-periodic harmonic systems. In previous papers (Benoit 1987, 1989) we have shown that infrared, Raman and inelastic neutron scattering spectra could be obtained from the following relations:

$$g(u) = -(1/\pi) \lim_{\varepsilon \to 0_+} \mathrm{Im}[R(z)]\} \tag{A1}$$

with $u = \omega^2$, $z = u + \mathrm{i}\varepsilon$ and

$$R(z) = \langle q | (z\mathbf{I} - \mathbf{D})^{-1} | q \rangle \tag{A2}$$

where $\mathbf{D}$ is the dynamical matrix and $|q\rangle$ is a vector which depends on the type of process studied and is assumed to be known. For instance the components of $|q\rangle$ are ionic charges if we study the infrared absorption. Now, if we consider (A2), we observe that $R(z)$ is just the scalar product of $|q\rangle$ with a vector $|x\rangle$ such that

$$(z\mathbf{I} - \mathbf{D})|x\rangle = |q\rangle. \tag{A3}$$

Equation (A3) represents a system of linear equations. It is a classical well known problem. Here $(z\mathbf{I} - \mathbf{D})$ is a complex and sparse matrix; so it is necessary to adapt programs. We have used the Crout reduction of the Gauss–Jordan L-R decomposition method (Isaacson and Keller 1966). With the model used here where the matrix is tridiagonal, the method is straightforward, the diagonal elements never being equal to zero from the analytic continuation in (A1). The results show that, as it is necessary to calculate $|x\rangle$ for every frequency, this method requires much more computer time than moment methods do. However, this method can be more accurate than the moment methods particularly in the low-frequency part of the spectrum.

We have used this procedure to check the convergence of the spectral moments method for systems with $N \leqslant 10\,000$ atoms. As for the moments method the scattering cross section is obtained in terms of ω by setting

$$\varepsilon = 2\gamma\omega \tag{A4}$$

which gives a constant width in the spectrum and by multiplying $g(u)$ by 2ω.

A2. Correlation functions

Another possibility of the direct inversion method is the determination of the Fourier transform of the displacement–displacement correlation function $G(n, n', \omega)$.

The displacement–displacement correlation function is given by (Maradudin 1969)

$$G(n, n', t) = \langle u_n(t) u_{n'}(0) \rangle$$

$$= \sum_j \frac{e_j(n) e_j(n')}{\sqrt{m_n}\sqrt{m_{n'}}} \frac{1}{2\omega_j} [(n_j + 1)\exp(-\mathrm{i}\omega_j t) + n_j \exp(\mathrm{i}\omega_j t)] \tag{A5}$$

where $\langle\ \rangle$ means that the statistical average is taken.

Now we consider the Fourier transforms of $G(n, n', t)$:

$$G(n, n', \omega) = \frac{1}{2\pi}\int \langle u_n(t)u_{n'}(0)\rangle \exp(i\omega t)\,dt$$

$$= \sum_j \frac{e_j(n)e_j(n')}{\sqrt{m_n}\sqrt{m_{n'}}}\frac{1}{2\omega_j}[(n_j+1)\delta(\omega-\omega_j)+n_j\delta(\omega+\omega_j)]. \tag{A6}$$

We consider the correlation function only for $\omega > 0$ and $T \to 0$. So it is equivalent to calculate a function G' which is identical with $G(n, n', \omega)$ for $\omega > 0$ and $T \to 0$ but it is symmetrical. The interest in this change is that G' is a function of the square of the frequency and we can work directly with the dynamical matrix:

$$G'(n, n', \omega) = \sum_j \frac{e_j(n)e_j(n')}{\sqrt{m_n}\sqrt{m_{n'}}}\frac{1}{2\omega_j}[\delta(\omega-\omega_j)+\delta(\omega+\omega_j)].$$

when $\lambda_j = \omega_j^2$,

$$G'(n, n', \omega) = \sum_j \frac{e_j(n)e_j(n')}{\sqrt{m_n}\sqrt{m_{n'}}}\delta(u-\lambda_j) \tag{A7}$$

$$= -\frac{1}{\pi}\lim\left[\mathrm{Im}\left(\sum_j \frac{e_j(n)e_j(n')}{\sqrt{m_n}\sqrt{m_{n'}}}\langle j|(z\mathbf{I}-\mathbf{D})^{-1}|j\rangle\right)\right]. \tag{A8}$$

Using Dirac bracket formalism

$$\langle n|j\rangle = e_j(n) \qquad \mathbf{D}|j\rangle = \lambda_j|j\rangle$$

one obtains

$$G'(n, n', \omega) = -\frac{1}{\pi\sqrt{m_n}\sqrt{m_{n'}}}\lim\{\mathrm{Im}[R_{n,n'}(z)]\} \tag{A9}$$

with

$$R_{n,n'}(z) = \langle n|(z\mathbf{I}-\mathbf{D})^{-1}|n'\rangle. \tag{A10}$$

Equation (A9) shows that $R_{n,n'}(z)$ is the scalar product of the vector $\langle n|$, which has only one component different from zero, with the vector $|y\rangle$ such that

$$|n'\rangle = (z\mathbf{I}-\mathbf{D})^{-1}|y\rangle \tag{A11}$$

where the vector $|n'\rangle$ is known. Hence one uses the same method as for $R(z)$.

References

Aubry S and Andre G 1979 *Proc. Israel Physical Society* vol 3, ed C G Kuper (Bristol: Hilger) p 133

Benoit C 1987 *J. Phys. C: Solid State Phys.* **20** 765

—— 1989 *J. Phys.: Condens. Matter* **1** 335

Benoit C and Poussigue G 1989 *High Performance Computing* ed J L Delaye and E Gelenbe (Amsterdam: North-Holland) p 347

Brockhouse B N 1966 *Phonons in Perfect Lattices and in Lattices with Point Imperfections* ed RWH Stevenson (Edinburgh: Oliver and Boyd)

Currat R and Janssen T 1988 *Solid State Phys.* **41** (New York: Academic) p 201

de Lange C and Janssen T 1981 *J. Phys. C: Solid State Phys.* **14** 5269

Glauber R J 1955 *Phys. Rev.* **98** 1692

Gratias D and Michel L 1986 *J. Physique* **47** C3

Isaacson E and Keller H B (ed) 1966 *Analysis of Numerical Methods* (New York: Wiley)

Janot C, Currat R and de Boissieu M 1988 private communication
Janot C and Dubois J M (ed) 1988 *Proc. ILL–CODEST Workshop on Quasicrystalline Materials* (Singapore: World Scientific)
Janssen T 1988a *Phys. Rep.* **168** 55
—— 1988b *Proc. ILL–CODEST Workshop on Quasicrystalline Materials* ed C Janot and J M Dubois (Singapore: World Scientific) p 327
Janssen T and Kohmoto M 1988 *Phys. Rev.* B **38** 5811
Kohmoto M 1983 *Phys. Rev. Lett.* **51** 119
Kohmoto M 1988 *Phys. Rev.* A **37** 1345
Kohmoto M and Banavar R 1986 *Phys. Rev.* B **34** 563
Kollar J and Suto A 1986 *Phys. Lett.* **117A** 203
Lu J P and Birman J L 1986 *J. Physique* **47** C3 251
Lu J P, Odagaki T and Birman J L 1986 *Phys. Rev.* B **33** 4809
Luck J M 1986 *J. Physique* **47** C3 205
Luck J M and Petritis D 1986 *J. Stat. Phys.* **42** 289
Maradudin A A 1969 *Lattice Dynamics. Progress in Physics* (New York: W A Benjamin) p 332
Ostlund S and Pandit R 1984 *Phys. Rev.* B **29** 1394
Shechtman D and Blech I A 1985 *Metall. Trans.* A **16** 1005
Shechtman D, Blech I A, Gratias D and Cahn J W 1984 *Phys. Rev. Lett.* **53** 1951
Van Hove L 1954 *Phys. Rev.* **95** 249
Walker C B 1956 *Phys. Rev.* **103** 547